Appropriate conditions to realize a p-wave superfluid state starting from a spin-orbit-coupled s-wave superfluid Fermi gas

T. Yamaguchi, D. Inotani, and Y. Ohashi
Department of Physics, Keio University, 3-14-1 Hiyoshi, Kohoku-ku, Yokohama 223-8522, Japan
(Received 27 January 2017; published 9 May 2017)

We theoretically investigate a spin-orbit-coupled s-wave superfluid Fermi gas, to examine the time evolution of the system, after an s-wave pairing interaction is replaced by a p-wave one at $t = 0$. In our recent paper [T. Yamaguchi, D. Inotani, and Y. Ohashi, J. Phys. Soc. Jpn. **86**, 013001 (2017)], we proposed that this manipulation may realize a p-wave superfluid Fermi gas because the p-wave pair amplitude that is induced in the s-wave superfluid state by a parity-broken antisymmetric spin-orbit interaction gives a nonvanishing p-wave superfluid order parameter, immediately after the p-wave interaction is turned on. In this paper, using a time-dependent Bogoliubov-de Gennes theory, we assess this idea under various conditions with respect to the s-wave and p-wave interaction strengths, as well as the spin-orbit coupling strength. From these, we clarify that the momentum distribution of Fermi atoms in the initial s-wave state ($t < 0$) is a key to produce a large p-wave superfluid order parameter. Since the realization of a p-wave superfluid state is one of the most exciting and difficult challenges in cold Fermi gas physics, our results may provide a possible way to accomplish this.

DOI: 10.1103/PhysRevA.95.053609

I. INTRODUCTION

In a recent letter [1], we proposed an idea to achieve a p-wave superfluid state in an ultracold Fermi gas. This proposal was strongly motivated by the current experimental difficulty that a p-wave pairing interaction, which is necessary to form p-wave Cooper pairs, also destroys the system before the p-wave condensate grows [2–6]. Because of this dilemma, the ordinary approach (that one cools a p-wave interacting Fermi gas down to the superfluid phase transition temperature) does not work at all. As a result, although p-wave Feshbach resonances have already been discovered in ^{40}K and ^{6}Li Fermi gases [7–15], the experimentally accessible superfluid state is still only the simplest s-wave type [16–19]. To demonstrate the usefulness of the cold Fermi gas system as a quantum simulator for various quantum many-body phenomena, the realization of a p-wave superfluid Fermi gas would be important. Since there are various p-wave Fermi superfluids, such as superfluid liquid ^{3}He [20,21], heavy-fermion superconductors [22–24], as well as a neutron condensate in a neutron star [25], a p-wave superfluid Fermi gas with a tunable pairing interaction would help further understandings of these unconventional Fermi superfluids. In cold Fermi gas physics, it is also interesting to see how the BCS (Bardeen-Cooper-Schrieffer)-BEC (Bose-Einstein condensation) crossover phenomenon discussed in an s-wave interacting Fermi gas [26–34] is extended to a p-wave one [35–40].

The key of our idea [1] is to *separately* prepare a p-wave Cooper-pair amplitude $\Phi_p^{\sigma\sigma'}(\boldsymbol{p}) = \langle c_{\boldsymbol{p},\sigma} c_{-\boldsymbol{p},\sigma'} \rangle$ and p-wave interaction $g_p(\boldsymbol{p},\boldsymbol{p}')$, both of which are involved in the p-wave superfluid order parameter,

$$\Delta_p^{\sigma\sigma'}(\boldsymbol{p}) = \sum_{\boldsymbol{p}'} g_p(\boldsymbol{p},\boldsymbol{p}')\Phi_p^{\sigma\sigma'}(\boldsymbol{p}'), \tag{1}$$

where $c_{\boldsymbol{p},\sigma}$ is the annihilation operator of a Fermi atom with pseudospins σ, describing atomic hyperfine states contributing to the pair formation. That is, the p-wave pair amplitude $\Phi_p^{\sigma\sigma'}(\boldsymbol{p})$ is first prepared by using an s-wave superfluid Fermi gas with an antisymmetric spin-orbit interaction. A recent synthetic gauge field technique has realized such a spin-orbit coupling in ultracold atomic gases [41–45]. At this stage, the system does not suffer from the above-mentioned damage caused by a p-wave interaction because the system only has an s-wave interaction. The p-wave superfluid Fermi gas is then immediately obtained by replacing the s-wave interaction with an appropriate p-wave one, where the p-wave superfluid order parameter $\Delta_p^{\sigma\sigma'}(\boldsymbol{p})$ in Eq. (1) is given by the product of the introduced p-wave interaction and the p-wave pair amplitude $\Phi_p^{\sigma\sigma'}(\boldsymbol{p})$ that has already been produced in the s-wave superfluid state. Of course, once the p-wave interaction is turned on, as usual, the system would start to be damaged by the p-wave interaction. However, the advantage of this idea is that the p-wave pair amplitude has been prepared in advance, so that the p-wave superfluid order parameter discontinuously becomes finite *immediately* after the replacement of the s-wave interaction by the p-wave one. Then, by definition, the system is in the p-wave superfluid state, being characterized by this p-wave superfluid order parameter, at least just after the p-wave interaction is turned on (as long as the system damage by the same p-wave interaction is not serious). We briefly note that the s-wave superfluid order parameter vanishes after the s-wave interaction is turned off.

The purpose of this paper is to clarify when our recent proposal [1] really gives a p-wave superfluid state with a large p-wave superfluid order parameter. This work is very important to experimentally use this idea because Ref. [1] also shows that it does *not* always work. That is, under a certain condition, the produced p-wave superfluid soon vanishes within the time scale being shorter than the typical lifetime ($\tau_l = 5$–20 ms) [2–4] of the system by the three-body loss caused by a p-wave interaction. For our purpose, in this paper, we employ a time-dependent Bogoliubov–de Gennes (TD-BdG) theory at $T = 0$ to systematically examine the time evolution of the p-wave superfluid order parameter $\Delta_p^{\sigma\sigma'}(\boldsymbol{p})$ under various conditions with respect to the spin-orbit-coupling strength, as well as the s-wave and p-wave interaction strengths. We then clarify a key to obtain a large p-wave superfluid order parameter. We also explain

detailed numerical TD-BdG calculations, which was omitted in Ref. [1].

TD-BdG theory cannot deal with the three-body particle loss or the relaxation of the system to the ground state because it conserves the particle number, as well as the total energy. However, this simple approach is still useful for the study of the early stage ($t \ll \tau_l$) of the time evolution of the system, after the replacement of an s-wave pairing interaction by a p-wave one. In this paper, we implicitly focus on such a shorter time domain before the three-body particle loss becomes crucial.

This paper is organized as follows. In Sec. II, we present our formulation. We also explain how to numerically deal with TD-BdG. In Sec. III, we show the time evolution of the p-wave superfluid order parameter, after the s-wave pairing interaction is replaced by a p-wave one, under various conditions. Based on these results, we discuss the condition to obtain a large p-wave superfluid order parameter. Throughout this paper, we take $\hbar = k_B = 1$, and the system volume is taken to be unity, for simplicity. In addition, the Fermi energy ε_F, Fermi momentum k_F, and Fermi velocity v_F mean the quantities in a free Fermi gas with no spin-orbit interaction.

II. FORMULATION

We consider the protocol in Fig. 1: When $t < 0$, we first prepare an equilibrium ultracold Fermi gas at $T = 0$. This system has an s-wave pairing interaction (to produce the s-wave superfluid state) as well as a parity-broken antisymmetric spin-orbit interaction [to induce a p-wave pair amplitude $\Phi_p^{\sigma\sigma'}(\boldsymbol{p})$] that are both turned off at $t = 0$. At the same time, a p-wave pairing interaction is switched on. Immediately after this manipulation, the product of this p-wave interaction and the p-wave pair amplitude (which has been induced in the s-wave superfluid state) gives a nonvanishing p-wave superfluid order parameter in Eq. (1).

To theoretically deal with this protocol, we consider an s-wave superfluid Fermi gas described by the Hamiltonian,

$$H_s = \sum_{\boldsymbol{p},\sigma,\sigma'} \left[\xi_{\boldsymbol{p}}\delta_{\sigma,\sigma'} + h_{\rm so}^{\sigma,\sigma'}\right] c_{\boldsymbol{p},\sigma}^\dagger c_{\boldsymbol{p},\sigma'} - g_s \sum_{\boldsymbol{p},\boldsymbol{p}',\boldsymbol{q}} c_{\boldsymbol{p}+\frac{\boldsymbol{q}}{2},\uparrow}^\dagger c_{-\boldsymbol{p}+\frac{\boldsymbol{q}}{2},\downarrow}^\dagger c_{-\boldsymbol{p}'+\frac{\boldsymbol{q}}{2},\downarrow} c_{\boldsymbol{p}'+\frac{\boldsymbol{q}}{2},\uparrow}. \quad (2)$$

Here, $c_{\boldsymbol{p},\sigma}^\dagger$ is the creation operator of a Fermi atom with an atomic mass m and pseudospins $\sigma = \uparrow,\downarrow$, describing two atomic hyperfine states forming s-wave Cooper pairs. $\xi_{\boldsymbol{p}} = \varepsilon_{\boldsymbol{p}} - \mu = \boldsymbol{p}^2/(2m) - \mu$ is the kinetic energy of a Fermi atom, measured from the Fermi chemical potential μ. $-g_s(< 0)$ is a contact-type s-wave attractive interaction, which is assumed to be tunable by adjusting a Feshbach resonance. In Eq. (2),

$$h_{\rm so}^{\sigma,\sigma'} = \lambda p_z \sigma_x^{\sigma,\sigma'} \quad (3)$$

is a single-component spin-orbit interaction ($\lambda \geqslant 0$), where σ_x is the Pauli matrix. This type of spin-orbit interaction has recently been realized in ^{40}K and ^{6}Li Fermi gases by using a synthetic gauge field technique [41–45]. In this experimental situation, we briefly note that the Fermi operator $c_{\boldsymbol{p},\sigma}$ in Eq. (2) describes a dressed state by an atom-light coupling. Since Eq. (3) breaks the spatial inversion symmetry, the resulting parity-mixing effect induces the spin-triplet pair amplitude $\Phi_t^{\sigma\sigma'}(\boldsymbol{p})$ in the (spin-singlet) s-wave superfluid state [46–49].

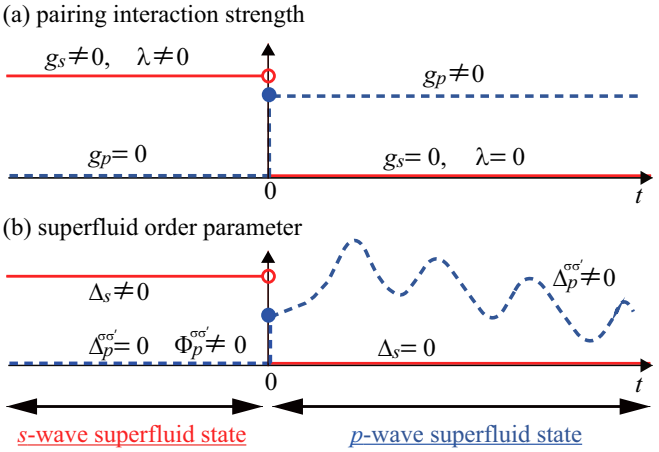

FIG. 1. (a) Proposed protocol to realize a p-wave superfluid Fermi gas. When $t < 0$, a p-wave pair amplitude $\Phi_p^{\sigma\sigma'}(\boldsymbol{p})$ is induced in an equilibrium s-wave superfluid Fermi gas with a parity-broken spin-orbit interaction ($\lambda \neq 0$). At this stage, while the system is still in the s-wave superfluid state with the s-wave superfluid order parameter $\Delta_s \neq 0$, the p-wave order parameter $\Delta_p^{\sigma\sigma'}(\boldsymbol{p})$ vanishes because of the vanishing p-wave interaction $g_p = 0$. At $t = 0$, we replace the s-wave interaction g_s with a p-wave one by adjusting an external magnetic field from an s-wave Feshbach-resonance field to a p-wave one ($g_s = 0$, $g_p \neq 0$). At the same time, we turn off the spin-orbit coupling $\lambda = 0$. The product of the p-wave pair amplitude $\Phi_p^{\sigma\sigma'}(\boldsymbol{p})$ which has been prepared in the parity-broken s-wave superfluid state and the introduced p-wave interaction g_p immediately gives a nonvanishing p-wave superfluid order parameter $\Delta_p^{\sigma\sigma'}(\boldsymbol{p}) \neq 0$. Then, by definition, the system is in the p-wave superfluid state. The s-wave superfluid order parameter vanishes ($\Delta_s = 0$) when $t \geqslant 0$ because the s-wave interaction is turned off (although the s-wave pair amplitude may remain). This p-wave superfluid state at $t \geqslant 0$ is generally not in the equilibrium state, so that $\Delta_p^{\sigma\sigma'}(\boldsymbol{p})$ may have time dependence, as schematically shown in (b).

Treating the model Hamiltonian in Eq. (2) within the BCS-Leggett theory at $T = 0$ [50,51], we consider the mean-field version of Eq. (2) having the form

$$H_s^{\rm MF} = \sum_{\boldsymbol{p},\sigma,\sigma'} \left[\xi_{\boldsymbol{p}}\delta_{\sigma,\sigma'} + h_{\rm so}^{\sigma,\sigma'}\right] c_{\boldsymbol{p},\sigma}^\dagger c_{\boldsymbol{p},\sigma'} + \Delta_s \sum_{\boldsymbol{p}} [c_{\boldsymbol{p},\uparrow}^\dagger c_{-\boldsymbol{p},\downarrow}^\dagger + \text{H.c.}], \quad (4)$$

where we have dropped an unimportant constant term. In Eq. (4), the s-wave superfluid order parameter,

$$\Delta_s = g_s \sum_{\boldsymbol{p}} \langle c_{\boldsymbol{p},\uparrow} c_{-\boldsymbol{p},\downarrow} \rangle, \quad (5)$$

obeys the ordinary BCS gap equation,

$$1 = -\frac{4\pi a_s}{m} \sum_{\boldsymbol{p}} \left[\frac{1}{2} \sum_{\alpha=\pm} \frac{1}{2E_{\boldsymbol{p}}^\alpha} - \frac{1}{2\varepsilon_{\boldsymbol{p}}} \right]. \quad (6)$$

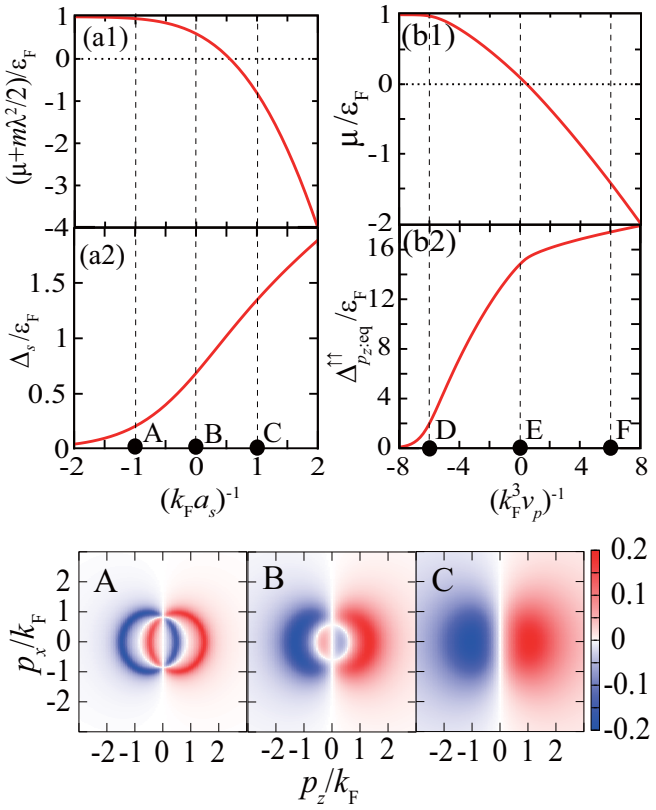

FIG. 2. (a1),(a2) BCS-Leggett solutions for a spin-orbit-coupled s-wave superfluid Fermi gas at $T = 0$. (a1) Fermi chemical potential μ. $\mu + m\lambda^2/2$ means the Fermi energy measured from the bottom of the energy band when $g_s = 0$. (a2) Calculated s-wave superfluid order parameter Δ_s. We take $\lambda/v_F = 0.5$. The lower three panels show the intensity of the spin-triplet Cooper-pair amplitude $\Phi_t^{\uparrow\uparrow}(p_x, p_y = 0, p_z)$ at A–C. (b1),(b2) BCS-Leggett solutions for an equilibrium p_z-wave superfluid Fermi gas when the basis function in Eq. (21) is given by $\boldsymbol{F}_{\boldsymbol{p}} = (0,0,F_{\boldsymbol{p}}^z)$. (b1) Fermi chemical potential μ. (b2) Calculated p_z-wave superfluid order parameter $\Delta^{\uparrow\uparrow}_{p_z:eq}$. The interaction strengths at A–C and D–F will be used as the initial s-wave interaction strengths ($t < 0$) and the p-wave interaction strengths ($t \geqslant 0$), respectively.

Here, $E_{\boldsymbol{p}}^{\pm} = \sqrt{(\xi_{\boldsymbol{p}}^{\pm})^2 + \Delta_s^2}$ describe Bogoliubov single-particle excitations in the presence of the spin-orbit coupling, where $\xi_{\boldsymbol{p}}^{\pm} = \xi_{\boldsymbol{p}} \pm \lambda|p_z|$. The ultraviolet divergence involved in the gap equation (6) has been absorbed into the s-wave scattering length a_s, which is related to the bare interaction $-g_s$ as [50–53]

$$\frac{4\pi a_s}{m} = -\frac{g_s}{1 - g_s \sum_{\boldsymbol{p}}^{p_c} 1/(2\varepsilon_{\boldsymbol{p}})}, \tag{7}$$

with p_c being a momentum cutoff. In the BCS-Leggett theory, one solves the gap equation (6), together with the equation for the number N of Fermi atoms,

$$N = \frac{1}{2}\sum_{\boldsymbol{p},\alpha=\pm}\left[1 - \frac{\xi_{\boldsymbol{p}}^{\alpha}}{E_{\boldsymbol{p}}^{\alpha}}\right], \tag{8}$$

to self-consistently determine Δ_s and μ. The calculated μ and Δ_s in the BCS-BEC crossover region are shown in Figs. 2(a1) and 2(a2), respectively. These results will be used in constructing the initial condition for the TD-BdG equation.

In our proposal [1], the role of the spin-orbit interaction $h_{so}^{\sigma,\sigma'}$ in Eq. (3) is to induce the spin-triplet Cooper-pair amplitudes,

$$\begin{aligned}
\Phi_t^{\uparrow\uparrow}(\boldsymbol{p}) &= \langle c_{\boldsymbol{p},\uparrow} c_{-\boldsymbol{p},\uparrow}\rangle = -\frac{p_z}{|p_z|}\sum_{\alpha=\pm}\alpha\frac{\Delta_s}{4E_{\boldsymbol{p}}^{\alpha}},\\
\Phi_t^{\uparrow\downarrow}(\boldsymbol{p}) &= \frac{1}{2}[\langle c_{\boldsymbol{p},\uparrow} c_{-\boldsymbol{p},\downarrow}\rangle + \langle c_{\boldsymbol{p},\downarrow} c_{-\boldsymbol{p},\uparrow}\rangle] = 0,\\
\Phi_t^{\downarrow\downarrow}(\boldsymbol{p}) &= \langle c_{\boldsymbol{p},\downarrow} c_{-\boldsymbol{p},\downarrow}\rangle = \frac{p_z}{|p_z|}\sum_{\alpha=\pm}\alpha\frac{\Delta_s}{4E_{\boldsymbol{p}}^{\alpha}},
\end{aligned} \tag{9}$$

without a p-wave interaction. For clarity, we explicitly show the momentum dependence of $\Phi_t^{\uparrow\uparrow}(\boldsymbol{p})$ in the lower panels in Fig. 2. We briefly note that $\Phi_t^{\sigma\sigma}(\boldsymbol{p})$ in Eq. (9) vanishes when $\lambda = 0$ because $E_{\boldsymbol{p}}^{+}(\lambda = 0) = E_{\boldsymbol{p}}^{-}(\lambda = 0)$. We also note that in spite of the presence of spin-triplet pair amplitudes $\Phi_t^{\sigma\sigma}(\boldsymbol{p}) \neq 0$, the p-wave superfluid order parameter is still absent because of the vanishing p-wave interaction. The spin-singlet pair amplitude,

$$\Phi_s^{\uparrow\downarrow}(\boldsymbol{p}) = \frac{1}{2}[\langle c_{\boldsymbol{p},\uparrow} c_{-\boldsymbol{p},\downarrow}\rangle - \langle c_{\boldsymbol{p},\downarrow} c_{-\boldsymbol{p},\uparrow}\rangle] = \sum_{\alpha=\pm}\frac{\Delta_s}{4E_{\boldsymbol{p}}^{\alpha}}, \tag{10}$$

only gives the nonvanishing s-wave superfluid order parameter, $\Delta_s = g_s\sum_{\boldsymbol{p}}\Phi_s^{\uparrow\downarrow}(\boldsymbol{p})$, which, of course, equals Eq. (5).

We use this equilibrium s-wave superfluid state as the initial state for the time evolution of the system after the s-wave interaction g_s is replaced by an appropriate p-wave one. For this purpose, it is convenient to reformulate the above equilibrium BCS-Leggett theory by using the time-dependent Bogoliubov–de Gennes (TD-BdG) equation [54–85],

$$i\frac{\partial}{\partial t}\tilde{\boldsymbol{\Psi}}(\boldsymbol{p},t) = \hat{H}_s^{\text{TD-BdG}}(t)\tilde{\boldsymbol{\Psi}}(\boldsymbol{p},t). \tag{11}$$

[The outline of the derivation of Eq. (11) is explained in Appendix A.] Here, the 4×4-matrix Hamiltonian $\hat{H}_s^{\text{TD-BdG}}$ corresponding to Eq. (4) is given by

$$\hat{H}_s^{\text{TD-BdG}}(t) = \begin{pmatrix} \varepsilon_{\boldsymbol{p}} & \lambda p_z & 0 & \tilde{\Delta}_s(t)\\ \lambda p_z & \varepsilon_{\boldsymbol{p}} & -\tilde{\Delta}_s(t) & 0\\ 0 & -\tilde{\Delta}_s^*(t) & -\varepsilon_{\boldsymbol{p}} & \lambda p_z\\ \tilde{\Delta}_s^*(t) & 0 & \lambda p_z & -\varepsilon_{\boldsymbol{p}} \end{pmatrix}. \tag{12}$$

In the TD-BdG equation (11), the four-component wave function,

$$\tilde{\boldsymbol{\Psi}}(\boldsymbol{p},t) = \begin{pmatrix} \tilde{u}_{\boldsymbol{p},\uparrow}^{\alpha}(t)\\ \tilde{u}_{\boldsymbol{p},\downarrow}^{\alpha}(t)\\ \tilde{v}_{\boldsymbol{p},\uparrow}^{\alpha}(t)\\ \tilde{v}_{\boldsymbol{p},\downarrow}^{\alpha}(t) \end{pmatrix}, \tag{13}$$

consists of the coefficients in the Bogoliubov transformation,

$$c_{\boldsymbol{p},\sigma}(t) = \sum_{\alpha=\pm}\left[\tilde{u}_{\boldsymbol{p},\sigma}^{\alpha}(t)\gamma_{\boldsymbol{p},\alpha} + \tilde{v}_{-\boldsymbol{p},\sigma}^{\alpha *}(t)\gamma_{-\boldsymbol{p}\alpha}^{\dagger}\right]. \tag{14}$$

Here, $\alpha = \pm$ represent two positive-energy eigenstates of the Hamiltonian $\hat{H}_s^{\text{TD-BdG}}(t)$ in Eq. (12) [86]. Imposing the

normalization condition, $|\tilde{u}^{\alpha}_{\boldsymbol{p},\sigma}(t)|^2 + |\tilde{v}^{\alpha}_{\boldsymbol{p},\sigma}(t)|^2 = 1$, one finds that the Bogoliubov operator $\gamma_{\boldsymbol{p},\alpha}$ obeys the Fermi statistics. The time-dependent superfluid order parameter $\tilde{\Delta}_s(t)$ in TD-BdG theory is given by

$$\tilde{\Delta}_s(t) = \frac{g_s}{2} \sum_{\boldsymbol{p},\alpha=\pm} \tilde{u}^{\alpha}_{\boldsymbol{p},\uparrow}(t)\tilde{v}^{\alpha *}_{\boldsymbol{p},\downarrow}(t). \tag{15}$$

In this scheme, the equilibrium mean-field BCS solutions (Δ_s,μ) at $T = 0$ [that are determined from the coupled gap equation (6) with the number equation (8)] are obtained as the steady-state solutions for Eq. (11), given by $\tilde{\Delta}_s(t) = e^{-2i\mu t}\Delta_s$, and

$$\tilde{\boldsymbol{\Psi}}(\boldsymbol{p},t) = e^{-iE^{\alpha}_{\boldsymbol{p}}t} \begin{pmatrix} e^{-i\mu t}u^{\alpha}_{\boldsymbol{p},\uparrow} \\ e^{-i\mu t}u^{\alpha}_{\boldsymbol{p},\downarrow} \\ e^{i\mu t}v^{\alpha}_{\boldsymbol{p},\uparrow} \\ e^{i\mu t}v^{\alpha}_{\boldsymbol{p},\downarrow} \end{pmatrix}. \tag{16}$$

Substituting these into Eq. (11), the ordinary (time-independent) Bogoliubov–de Gennes (BdG) equation [87] is reproduced as

$$\begin{pmatrix} \xi_{\boldsymbol{p}} & \lambda p_z & 0 & \Delta_s \\ \lambda p_z & \xi_{\boldsymbol{p}} & -\Delta_s & 0 \\ 0 & -\Delta_s & -\xi_{\boldsymbol{p}} & \lambda p_z \\ \Delta_s & 0 & \lambda p_z & -\xi_{\boldsymbol{p}} \end{pmatrix} \boldsymbol{\Psi}^{\alpha}_s(\boldsymbol{p}) = E^{\alpha}_{\boldsymbol{p}} \boldsymbol{\Psi}^{\alpha}_s(\boldsymbol{p}). \tag{17}$$

For the eigenenergy $E^{\alpha}_{\boldsymbol{p}}$ given below Eq. (6), the eigenfunction has the form

$$\boldsymbol{\Psi}^{\alpha}_s(\boldsymbol{p}) = \begin{pmatrix} u^{\alpha}_{\boldsymbol{p},\uparrow} \\ u^{\alpha}_{\boldsymbol{p},\downarrow} \\ v^{\alpha}_{\boldsymbol{p},\uparrow} \\ v^{\alpha}_{\boldsymbol{p},\downarrow} \end{pmatrix} = \frac{1}{\sqrt{2}} \begin{pmatrix} \sqrt{1 + \frac{\xi^{\alpha}_{\boldsymbol{p}}}{E^{\alpha}_{\boldsymbol{p}}}} \\ \alpha \frac{p_z}{|p_z|}\sqrt{1 + \frac{\xi^{\alpha}_{\boldsymbol{p}}}{E^{\alpha}_{\boldsymbol{p}}}} \\ -\alpha \frac{p_z}{|p_z|}\sqrt{1 - \frac{\xi^{\alpha}_{\boldsymbol{p}}}{E^{\alpha}_{\boldsymbol{p}}}} \\ \sqrt{1 - \frac{\xi^{\alpha}_{\boldsymbol{p}}}{E^{\alpha}_{\boldsymbol{p}}}} \end{pmatrix}. \tag{18}$$

This BdG solution reproduces the gap equation (6), as well as the number equation (8), from the ordinary expressions in the BCS theory,

$$\Delta_s = \frac{g_s}{2} \sum_{\boldsymbol{p},\alpha=\pm} u^{\alpha}_{\boldsymbol{p},\uparrow} v^{\alpha}_{\boldsymbol{p},\downarrow},$$
$$N = \frac{1}{2} \sum_{\boldsymbol{p},\sigma,\alpha=\pm} \left|v^{\alpha}_{\boldsymbol{p},\sigma}\right|^2. \tag{19}$$

We will use $\tilde{\boldsymbol{\Psi}}(\boldsymbol{p},t=0) = \boldsymbol{\Psi}^{\alpha}_s(\boldsymbol{p})$ in Eqs. (16) and (18) as the initial state in considering the time evolution of the system when $t \geqslant 0$.

At $t = 0$, we replace the s-wave interaction in Eq. (2) by an appropriate p-wave one. For simplicity, we also switch off the spin-orbit interaction ($\lambda = 0$) at the same time. For example, an ultracold ^{40}K Fermi gas consisting of two atomic hyperfine states, $|F,F_z\rangle = |9/2,-7/2\rangle(\equiv|\uparrow\rangle)$ and $|9/2,-9/2\rangle(\equiv|\downarrow\rangle)$, has a p-wave Feshbach resonance between atoms in $|\uparrow\rangle$ at $B_p = 199$ G, in addition to an s-wave Feshbach resonance at $B_s = 202$ G [8,16] between $|\uparrow\rangle$ and $|\downarrow\rangle$ (where $F = I + S$, with I and S being a nuclear spin and electron spin, respectively). In this case, our attempt is achieved by adjusting an external magnetic field from B_s to B_p [3,4,6,10–15]. Strictly speaking, although a weak s-wave interaction may still remain finite even near the p-wave Feshbach resonance, we ignore this effect, for simplicity.

We consider the case when the s-wave pairing interaction in the last term in Eq. (2) is suddenly replaced by the p-wave one between $\uparrow$-spin atoms [35–38], given by

$$V_p = -\frac{g_p}{2} \sum_{\boldsymbol{p},\boldsymbol{p}',\boldsymbol{q}} \boldsymbol{F}_{\boldsymbol{p}} \cdot \boldsymbol{F}_{\boldsymbol{p}'} c^{\dagger}_{\boldsymbol{p}+\frac{\boldsymbol{q}}{2},\uparrow} c^{\dagger}_{-\boldsymbol{p}+\frac{\boldsymbol{q}}{2},\uparrow} c_{-\boldsymbol{p}'+\frac{\boldsymbol{q}}{2},\uparrow} c_{\boldsymbol{p}'+\frac{\boldsymbol{q}}{2},\uparrow}. \tag{20}$$

Here,

$$\boldsymbol{F}_{\boldsymbol{p}} = \frac{\boldsymbol{p}\, p_0}{\boldsymbol{p}^2 + p_0^2} \tag{21}$$

is a p-wave basis function [35], where p_0 is a cutoff momentum, which we take as $p_0 = 10k_{\mathrm{F}} \gg k_{\mathrm{F}}$ in this paper [88,89]. In Eq. (20), we simply assume an isotropic p-wave interaction, although a realistic p-wave interaction associated with a Feshbach resonance may be anisotropic [8]. In this regard, as will be shown in Eq. (24), the p_z-wave component in Eq. (20) only contributes to the p-wave superfluid order parameter in the present case. Thus, this simplification is actually not so crucial in the following discussions.

The p-wave coupling constant g_p is related to the observable p-wave scattering volume v_p as [35]

$$\frac{4\pi v_p p_0^2}{m} = -\frac{g_p/3}{1 - (g_p/3)\sum_{\boldsymbol{p}} \boldsymbol{F}^2_{\boldsymbol{p}}/(2\varepsilon_{\boldsymbol{p}})}. \tag{22}$$

As usual, we measure the p-wave interaction strength in terms of $(k_{\mathrm{F}}^3 v_p)^{-1}$ [35–38]. In this scale, the weak-coupling side and the strong-coupling side are characterized as $(k_{\mathrm{F}}^3 v_p)^{-1} \lesssim 0$ and $(k_{\mathrm{F}}^3 v_p)^{-1} \gtrsim 0$, respectively.

We briefly note that in the present case, the $\downarrow$-spin component becomes a noninteracting Fermi gas when $t \geqslant 0$.

We also note that although the s-wave superfluid order parameter $\Delta_s = g_s \sum_{\boldsymbol{p}} \langle c_{\boldsymbol{p},\uparrow} c_{-\boldsymbol{p},\downarrow}\rangle$ vanishes when the s-wave interaction g_s is turned off at $t = 0$, the spin-triplet pair amplitude $\Phi_{\mathrm{t}}^{\sigma\sigma}(\boldsymbol{p})$ in Eq. (9) remains finite, although Eq. (9) looks vanishing when $\Delta_s(t \geqslant 0) = 0$. To see this in a simple manner, it is convenient to assume that all the interactions are turned off when $t \geqslant 0$. In this extreme case, TD-BdG equation (11) [with $\lambda = 0$ and $\tilde{\Delta}_s(t) = 0$] gives the analytic solution ($t \geqslant 0$),

$$\boldsymbol{\Psi}^{\alpha}_{\mathrm{free}}(\boldsymbol{p},t) = \begin{pmatrix} e^{-i\varepsilon_{\boldsymbol{p}}t}u^{\alpha}_{\boldsymbol{p},\uparrow} \\ e^{-i\varepsilon_{\boldsymbol{p}}t}u^{\alpha}_{\boldsymbol{p},\downarrow} \\ e^{i\varepsilon_{\boldsymbol{p}}t}v^{\alpha}_{\boldsymbol{p},\uparrow} \\ e^{i\varepsilon_{\boldsymbol{p}}t}v^{\alpha}_{\boldsymbol{p},\downarrow} \end{pmatrix}, \tag{23}$$

where we have set the initial condition as $\tilde{\boldsymbol{\Psi}}(\boldsymbol{p},t=0) = \boldsymbol{\Psi}^{\alpha}_s(\boldsymbol{p})$ given in Eq. (18). Equation (23) gives the nonvanishing spin-triplet pair amplitude $\Phi_{\mathrm{t}}^{\sigma\sigma}(\boldsymbol{p},t)$ in Eq. (9) at arbitrary $t \geqslant 0$.

Thus, when the s-wave pairing interaction is replaced by the p-wave one V_p in Eq. (20), the product of this introduced

p-wave interaction and the spin-triplet pair amplitude $\Phi_{\rm t}^{\uparrow\uparrow}(\boldsymbol{p})$ immediately gives the nonvanishing p_z-wave superfluid order parameter at $t=0$, given by

$$\Delta_{p_z}^{\uparrow\uparrow}(\boldsymbol{p},t=0)=g_pF_{\boldsymbol{p}}^z\sum_{\boldsymbol{p}'}F_{\boldsymbol{p}'}^z\Phi_{\rm t}^{\uparrow\uparrow}(\boldsymbol{p}',t=0)$$
$$=-g_pF_{\boldsymbol{p}}^z\sum_{\boldsymbol{p}',\alpha=\pm}\frac{|p_z'|p_0}{\boldsymbol{p}'^2+p_0^2}\alpha\frac{\Delta_s}{4E_{\boldsymbol{p}'}^\alpha}. \quad (24)$$

The p_x-wave and p_y-wave components $\Delta_{p_j}^{\uparrow\uparrow}(\boldsymbol{p})=g_pF_{\boldsymbol{p}}^j\sum_{\boldsymbol{p}'}F_{\boldsymbol{p}'}^j\langle c_{\boldsymbol{p}',\uparrow}c_{-\boldsymbol{p}',\uparrow}\rangle$ $(j=x,y)$ are not produced at $t=0$ because of the absence of the corresponding spin-triplet pair amplitudes. Thus, as usual, these two components start to grow from zero when $t\geqslant 0$. However, the current experimental difficulty indicates that the time scale of such condensation growth [6,90] is considered to be much longer than the typical lifetime ($\tau_{\rm l}=5$–20 ms) of a p-wave interacting Fermi gas [2–4]. Thus, the p_x-wave and p_y-wave superfluid state would actually be difficult in the present case. Since we consider the early stage ($t\ll\tau_{\rm l}$) of the time evolution of the system, we only retain the p_z-wave superfluid component in what follows.

Starting from the initial condition $\tilde{\boldsymbol{\Psi}}(\boldsymbol{p},t=0)=\boldsymbol{\Psi}_s^\alpha(\boldsymbol{p})$ in Eq. (18), we evaluate the time evolution of the wave function $\tilde{\boldsymbol{\Psi}}(\boldsymbol{p},t\geqslant 0)$, using TD-BdG equation (11) where $\hat{H}_s^{\rm TD\text{-}BdG}$ is replaced by

$$\hat{H}_p^{\rm TD\text{-}BdG}=\begin{pmatrix}\varepsilon_{\boldsymbol{p}} & 0 & \Delta_{p_z}^{\uparrow\uparrow}(\boldsymbol{p},t) & 0\\ 0 & \varepsilon_{\boldsymbol{p}} & 0 & 0\\ \Delta_{p_z}^{\uparrow\uparrow *}(\boldsymbol{p},t) & 0 & -\varepsilon_{\boldsymbol{p}} & 0\\ 0 & 0 & 0 & -\varepsilon_{\boldsymbol{p}}\end{pmatrix}. \quad (25)$$

Here, the time-dependent p_z-wave superfluid order parameter $\Delta_{p_z}^{\uparrow\uparrow}(\boldsymbol{p},t)$ at $t\geqslant 0$ is evaluated as

$$\Delta_{p_z}^{\uparrow\uparrow}(\boldsymbol{p},t)=\frac{g_p}{2}F_{\boldsymbol{p}}^z\sum_{\boldsymbol{p}',\alpha=\pm}F_{\boldsymbol{p}'}^z\tilde{u}_{\boldsymbol{p}',\uparrow}^\alpha(t)\tilde{v}_{\boldsymbol{p}',\uparrow}^{\alpha *}(t)$$
$$\equiv F_{\boldsymbol{p}}^z\Delta_{p_z}^{\uparrow\uparrow}(t). \quad (26)$$

Since the Hamiltonian $\hat{H}_p^{\rm TD\text{-}BdG}$ in Eq. (25) does not involve the Fermi chemical potential μ, we do not need to calculate the number equation $N(t)=(1/2)\sum_{\boldsymbol{p},\sigma,\alpha=\pm}|\tilde{v}_{\boldsymbol{p},\sigma}^\alpha(t)|^2$ at $t\geqslant 0$. The conservation of the particle number is guaranteed in TD-BdG theory.

Noting that the p-wave interacting $\uparrow$-spin component is decoupled from the $\downarrow$-spin component when $t\geqslant 0$, one may simplify the TD-BdG equation as

$$i\frac{\partial}{\partial t}\boldsymbol{\Phi}(\boldsymbol{p},t)=\begin{pmatrix}\varepsilon_{\boldsymbol{p}} & \Delta_{p_z}^{\uparrow\uparrow}(\boldsymbol{p},t)\\ \Delta_{p_z}^{\uparrow\uparrow *}(\boldsymbol{p},t) & -\varepsilon_{\boldsymbol{p}}\end{pmatrix}\boldsymbol{\Phi}(\boldsymbol{p},t)$$
$$\equiv\hat{H}_{p:2\times 2}^{\rm TD\text{-}BdG}\boldsymbol{\Phi}(\boldsymbol{p},t), \quad (27)$$

where $\boldsymbol{\Phi}(\boldsymbol{p},t)=(\tilde{u}_{\boldsymbol{p},\uparrow}^\alpha(t),\tilde{v}_{\boldsymbol{p},\uparrow}^\alpha(t))^T$.

Before ending this section, we give two notes on numerical calculations. The first one is how to numerically deal with TD-BdG equation (27). In computations, one needs to discretize the time variable with a finite interval Δt, which we take as $\Delta t=10^{-5}\varepsilon_{\rm F}^{-1}$ in this paper. In this case, the time evolution of the wave function $\boldsymbol{\Phi}(\boldsymbol{p},t)$, to the accuracy of $O((\Delta t)^2)$, is written as

$$\boldsymbol{\Phi}(\boldsymbol{p},t+\Delta t)\simeq\boldsymbol{\Phi}(\boldsymbol{p},t)+\frac{\partial\boldsymbol{\Phi}(\boldsymbol{p},t)}{\partial t}\Delta t+\frac{\partial^2\boldsymbol{\Phi}(\boldsymbol{p},t)}{\partial t^2}\frac{(\Delta t)^2}{2}$$
$$=\boldsymbol{\Phi}(\boldsymbol{p},t)-i\hat{H}_{p:2\times 2}^{\rm TD\text{-}BdG}(t)\boldsymbol{\Phi}(\boldsymbol{p},t)\Delta t$$
$$-\left\{i\frac{\partial\hat{H}_{p:2\times 2}^{\rm TD\text{-}BdG}(t)}{\partial t}+\left[\hat{H}_{p:2\times 2}^{\rm TD\text{-}BdG}(t)\right]^2\right\}$$
$$\times\boldsymbol{\Phi}(\boldsymbol{p},t)\frac{(\Delta t)^2}{2}. \quad (28)$$

However, when we naively use Eq. (28), the normalization of the wave function, $\boldsymbol{\Phi}(\boldsymbol{p},t)^\dagger\boldsymbol{\Phi}(\boldsymbol{p},t)=1$, is gradually broken with the passage of time. Thus, to cure this, we rewrite Eq. (28) into the product of the unitary operator,

$$\mathcal{U}(t,\Delta t)=e^{-i\hat{H}_{p:2\times 2}^{\rm TD\text{-}BdG}(t)\Delta t}, \quad (29)$$

as

$$\boldsymbol{\Phi}(\boldsymbol{p},t+\Delta t)=\mathcal{U}(t+b\Delta t,a_2\Delta t)\mathcal{U}(t,a_1\Delta t)\boldsymbol{\Phi}(t). \quad (30)$$

Here, a_1, a_2, and b are determined so that Eq. (30) can coincide with Eq. (28) within the accuracy of $O((\Delta t)^2)$. Expanding Eq. (30) in terms of Δt to the second order, one has

$$\boldsymbol{\Phi}(\boldsymbol{p},t+\Delta t)\simeq\boldsymbol{\Phi}(\boldsymbol{p},t)-i[a_1+a_2]\hat{H}_{p:2\times 2}^{\rm TD\text{-}BdG}(t)\boldsymbol{\Phi}(\boldsymbol{p},t)\Delta t$$
$$-\left\{i(2a_2b)\frac{\partial\hat{H}_{p:2\times 2}^{\rm TD\text{-}BdG}(t)}{\partial t}+[a_1+a_2]^2\right.$$
$$\left.\times\left[\hat{H}_{p:2\times 2}^{\rm TD\text{-}BdG}(t)\right]^2\right\}\boldsymbol{\Phi}(\boldsymbol{p},t)\frac{(\Delta t)^2}{2}. \quad (31)$$

Comparing Eq. (28) with Eq. (31), one finds

$$a_1+a_2=[a_1+a_2]^2=2a_2b=1. \quad (32)$$

As a solution of Eq. (32), we choose $a_1=a_2=1/2$ and $b=1$. The time evolution operator $\mathcal{U}(t,\Delta t)$ in Eq. (30) is conveniently written as

$$\mathcal{U}(t,\Delta t)=\cos[W_{\boldsymbol{p}}(t)\Delta t]-i\sin[W_{\boldsymbol{p}}(t)\Delta t]\frac{\hat{H}_{p:2\times 2}^{\rm TD\text{-}BdG}(t)}{W_{\boldsymbol{p}}(t)},$$
$$\left[W_{\boldsymbol{p}}(t)=\sqrt{\varepsilon_{\boldsymbol{p}}^2+|\Delta_{p_z}^{\uparrow\uparrow}(\boldsymbol{p},t)|^2}\right]. \quad (33)$$

The second note is about s-wave and p-wave interaction strengths. In the equilibrium s-wave state ($t<0$), we consider the three cases shown in Figs. 2(a1) and 2(a2): (A) $(k_{\rm F}a_s)^{-1}=-1$ (weak-coupling case where $\mu\sim\varepsilon_{\rm F}$), (B) $(k_{\rm F}a_s)^{-1}=0$ (intermediate-coupling case where $0<\mu<\varepsilon_{\rm F}$), and (C) $(k_{\rm F}a_s)^{-1}=1$ (strong-coupling case where $\mu<0$). For the p-wave interaction, we deal with the three cases denoted as D, E, and F in Figs. 2(b1) and 2(b2). In these figures, μ and $\Delta_{p_z:{\rm eq}}^{\uparrow\uparrow}(\boldsymbol{p})=F_{\boldsymbol{p}}^z\Delta_{p_z:{\rm eq}}^{\uparrow\uparrow}$ are, respectively, the chemical potential and the p_z-wave superfluid order parameter in the equilibrium p_z-wave superfluid phase. These quantities are

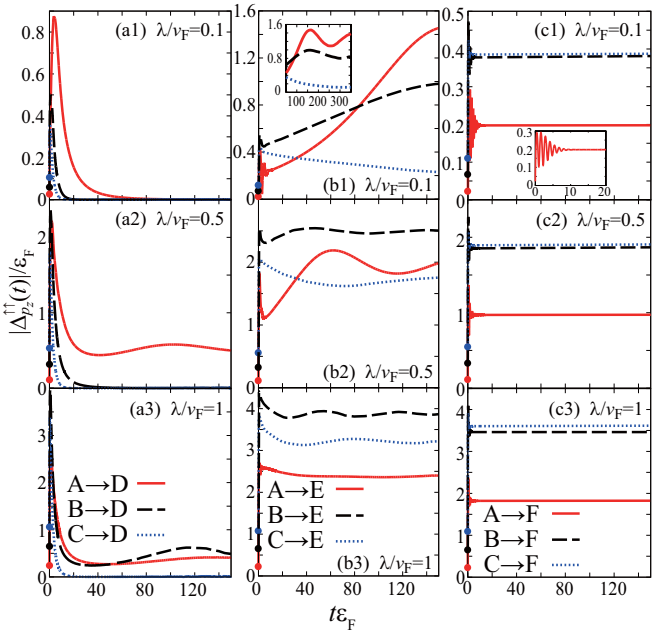

FIG. 3. Calculated time evolution of the magnitude of the p_z-wave superfluid order parameter $|\Delta^{\uparrow\uparrow}_{p_z}(t \geqslant 0)|$. The s-wave interaction strength ($t < 0$) and the p-wave interaction strength ($t \geqslant 0$) are shown as, for example, A → D. Here, A–C and D–F, respectively, represent the s-wave and p-wave interaction strengths shown in Fig. 2. The solid circles show $|\Delta^{\uparrow\uparrow}_{p_z}(t = 0)|$. The insets in (b1) and (c1) show the long-time and short-time behaviors of $|\Delta^{\uparrow\uparrow}_{p_z}(t)|$, respectively.

determined from the p_z-wave BCS-Leggett coupled equations,

$$1 = g_p \sum_{\boldsymbol{p}} \frac{(F^z_{\boldsymbol{p}})^2}{2\sqrt{\xi^2_{\boldsymbol{p}} + [\Delta^{\uparrow\uparrow}_{p_z:\mathrm{eq}}(\boldsymbol{p})]^2}},$$

$$N = \sum_{\boldsymbol{p}} \left\{ 1 - \frac{\xi_{\boldsymbol{p}}}{\sqrt{\xi^2_{\boldsymbol{p}} + [\Delta^{\uparrow\uparrow}_{p_z:\mathrm{eq}}(\boldsymbol{p})]^2}} \right\}. \tag{34}$$

As seen in Figs. 2(b1) and 2(b2), the case D $[(k_F^3 v_p)^{-1} = -6]$ is in the weak-coupling regime (where $\mu \sim \varepsilon_F$), the case E $[(k_F^3 v_p)^{-1} = 0]$ is in the intermediate-coupling regime (where $\mu \sim 0$), and the case F $[(k_F^3 v_p)^{-1} = 6]$ is in the strong-coupling regime where $\mu < 0$. Although the system is in the nonequilibrium state when $t \geqslant 0$, these equilibrium results are helpful to grasp their physical situations. In Sec. III, we will consider all the possible combinations between (A,B,C) and (D,E,F) to examine the time evolution of the system.

III. TIME EVOLUTION OF p_z-WAVE SUPERFLUID ORDER PARAMETER

Figure 3 shows the time evolution of the magnitude of the p_z-wave superfluid order parameter $|\Delta^{\uparrow\uparrow}_{p_z}(t \geqslant 0)|$ in Eq. (26) [91]. As expected, the nonvanishing $\Delta^{\uparrow\uparrow}_{p_z}(t)$ discontinuously appears at $t = 0$ (solid circles in Fig. 3). In addition, except for the case of a weak p-wave interaction (case D) in Figs. 3(a1)–3(a3), the p_z-wave superfluid order parameter $\Delta^{\uparrow\uparrow}_{p_z}(t)$ continues to exist even at $t\varepsilon_F = 100$. For the typical value $\varepsilon_F \sim 1\ \mu$K in an ultracold Fermi gas [16], the time

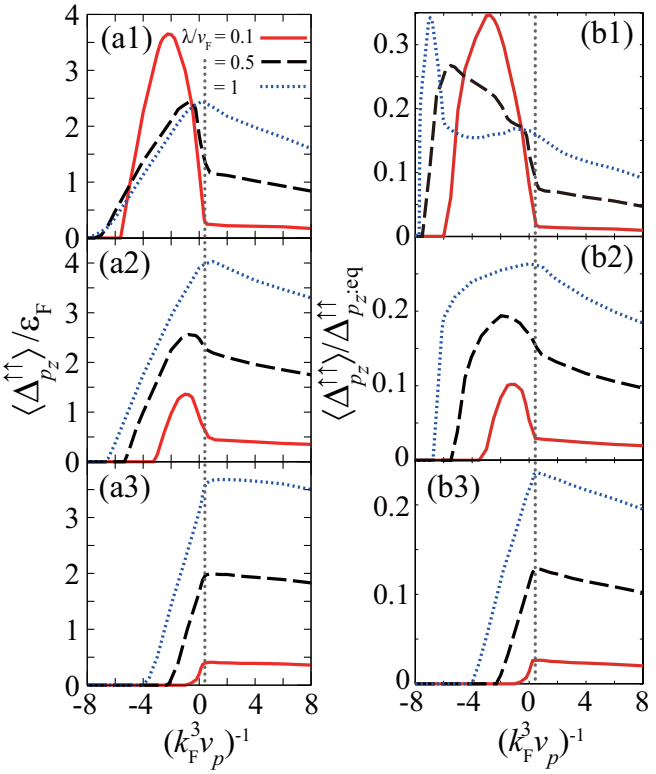

FIG. 4. (a1)–(a3) Time-averaged p_z-wave superfluid order parameter $\langle\Delta^{\uparrow\uparrow}_{p_z}\rangle$ in Eq. (35). The initial s-wave interaction strength is (a1) $(k_F a_s)^{-1} = -1$, (a2) $(k_F a_s)^{-1} = 0$, and (a3) $(k_F a_s)^{-1} = 1$. At the vertical dotted line $[(k_F^3 v_p)^{-1} = 0.447]$, the Fermi chemical potential μ changes its sign in the equilibrium p_z-wave superfluid state. (b1)–(b3) The same plots as (a1)–(a3), where $\langle\Delta^{\uparrow\uparrow}_{p_z}\rangle$ is normalized by the equilibrium value $\Delta^{\uparrow\uparrow}_{p_z:\mathrm{eq}}$.

scale $t\varepsilon_F = 1$ corresponds to $t = O(10^{-2}$ ms). We then find from the inset in Fig. 3(c1) that $\Delta^{\uparrow\uparrow}_{p_z}(t)$ increases with the short-time scale $t = O(10^{-2}$ ms), which means that the p_z-wave superfluid order parameter can grow enough before the three-body particle loss seriously damages the system ($\lesssim$5–20 ms) [2–6].

However, Figs. 3(a1)–3(a3) show that our idea does *not* always work, at least in the p-wave weak-coupling case (case D). In Fig. 3(a1), although $\Delta^{\uparrow\uparrow}_{p_z}(t)$ first rapidly increases just after the p_z-wave interaction is tuned on ($0 \leqslant t\varepsilon_F \lesssim 5$), it soon becomes small and vanishes (within the numerical accuracy). Such vanishing behavior of the p_z-wave superfluid order parameter tends to occur for smaller spin-orbit coupling λ, as well as stronger s-wave interaction g_s, as seen in Figs. 3(a1)–3(a3).

To quantify this vanishing behavior of $\Delta^{\uparrow\uparrow}_{p_z}(t)$ in a simple manner, we introduce the time-averaged superfluid order parameter, defined by [92]

$$\langle\Delta^{\uparrow\uparrow}_{p_z}\rangle = \frac{1}{50\varepsilon_F^{-1}} \int_{50\varepsilon_F^{-1}}^{100\varepsilon_F^{-1}} dt\, |\Delta^{\uparrow\uparrow}_{p_z}(t)|. \tag{35}$$

As shown in Figs. 4(a1)–4(a3), this averaged quantity always almost vanishes deep inside the weak-coupling regime $(k_F^3 v_p)^{-1} \ll -1$ (within the numerical accuracy). Even when

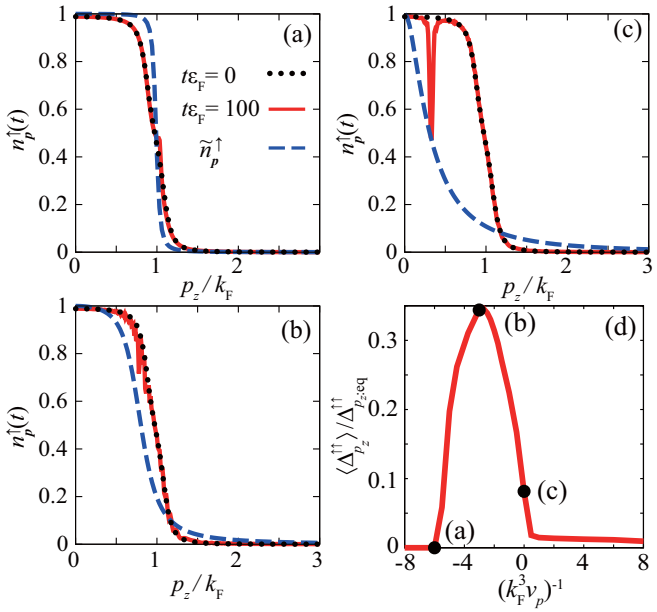

FIG. 5. Calculated momentum distribution function $n_{\boldsymbol{p}}^{\uparrow}(t)$ in the p_z-wave superfluid phase, given in Eq. (36). $\tilde{n}_{\boldsymbol{p}}^{\uparrow}$ is the equilibrium result, given in Eq. (37). We set $(k_F a_s)^{-1} = -1$, $\lambda/v_F = 0.1$, and $\boldsymbol{p} = (0,0,p_z)$. (a) $(k_F^3 v_p)^{-1} = -6$. (b) $(k_F^3 v_p)^{-1} = -3$. (c) $(k_F^3 v_p)^{-1} = 0$. (d) The magnitude of the averaged p_z-wave superfluid order parameter $\langle\Delta_{p_z}^{\uparrow\uparrow}\rangle$ in each case.

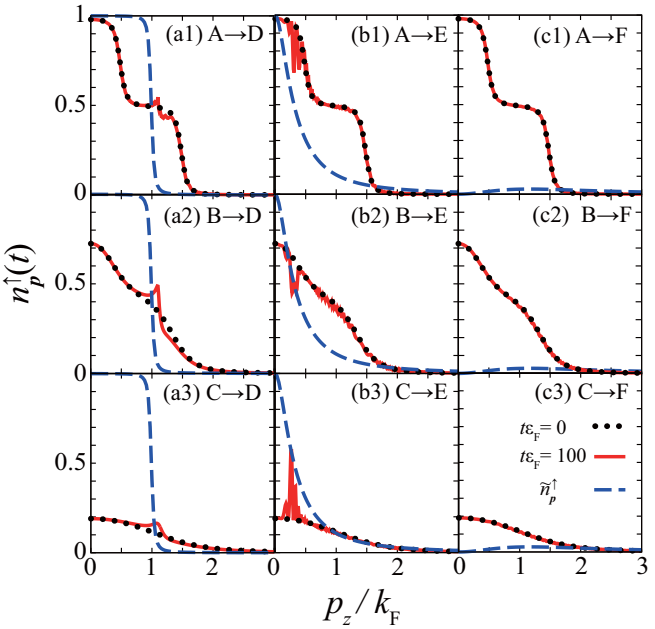

FIG. 6. Calculated atomic momentum distribution function $n_{\boldsymbol{p}}^{\uparrow}(t)$ with $\boldsymbol{p} = (0,0,p_z)$. We take $\lambda/v_F = 0.5$. $\tilde{n}_{\boldsymbol{p}}^{\uparrow}$ is the momentum distribution in the equilibrium case. The steplike structures seen around $p_z/k_F = 1$ in (a1)–(c1), reflect the momentum distribution in a spin-orbit-coupled Fermi gas.

$\langle\Delta_{p_z}^{\uparrow\uparrow}\rangle$ remains finite, it is found to be always smaller than $\Delta_{p_z:\mathrm{eq}}^{\uparrow\uparrow}$ in the equilibrium case [see Figs. 4(b1)–4(b3)], indicating that the superfluid order parameter is suppressed in the present nonequilibrium state.

To understand this nonequilibrium effect, it is useful to compare the momentum distribution function of the ↑-spin component,

$$n_{\boldsymbol{p}}^{\uparrow}(t) = \langle c_{\boldsymbol{p},\uparrow}^{\dagger}(t) c_{\boldsymbol{p},\uparrow}(t)\rangle = \frac{1}{2}\sum_{\alpha=\pm} \left|\tilde{v}_{\boldsymbol{p},\uparrow}^{\alpha}(t)\right|^2, \tag{36}$$

with that in the equilibrium p_z-wave state,

$$\tilde{n}_{\boldsymbol{p}}^{\uparrow} = \frac{1}{2}\left\{1 - \frac{\xi_{\boldsymbol{p}}}{\sqrt{\xi_{\boldsymbol{p}}^2 + [\Delta_{p_z:\mathrm{eq}}^{\uparrow\uparrow}(\boldsymbol{p})]^2}}\right\}. \tag{37}$$

In Fig. 5, we find that, apart from details, the overall structure of $n_{\boldsymbol{p}}^{\uparrow}(t)$ at $t\varepsilon_F = 100$ is almost the same as that at $t = 0$ [1]. This is because the present TD-BdG cannot describe the energy relaxation of the system to the ground state, so that the momentum distribution of Fermi atoms in the equilibrium s-wave superfluid state ($t < 0$) is almost passed down to the nonequilibrium p_z-wave state ($t \geqslant 0$). Indeed, this phenomenon is also seen in other cases, as shown in Fig. 6. In particular, as shown in Appendix B, the momentum distribution function $n_{\boldsymbol{p}}^{\uparrow}(t)$ in the nodal direction, $\boldsymbol{p} = (p_x, p_y, 0)$, is time independent. Judging from the current experiments for the realization of a p-wave superfluid Fermi gas [2–6], the time scale of the relaxation to the p-wave superfluid ground state seems much longer than the lifetime ($\tau_l = 5$–20 ms) of the system by the three-body particle loss. Thus, as far as we consider the early stage of the time evolution, $0 \leqslant t \ll \tau_l$ [$t\varepsilon_F \ll O(10^3)$], the atomic momentum distribution in the p_z-wave state would be similar to that in the initial s-wave state.

In Fig. 5(a), where $\langle\Delta_{p_z}^{\uparrow\uparrow}\rangle \simeq 0$ [see Fig. 5(d)], the Fermi edge in $n_{\boldsymbol{p}}^{\uparrow}(t)$ around $p_z/k_F = 1$ is more smeared than the equilibrium result, $\tilde{n}_{\boldsymbol{p}}^{\uparrow}$. When we replot the latter as a function of the kinetic energy $\varepsilon_{\boldsymbol{p}} = \boldsymbol{p}^2/(2m)$, the energy width $\delta\omega$ of the smearing of the Fermi edge is estimated as $\delta\omega \sim \Delta_{p_z:\mathrm{eq}}^{\uparrow\uparrow}$. On the other hand, the p_z-wave superfluid order parameter almost vanishes at $t\varepsilon_F = 100$ in the nonequilibrium case shown in Fig. 5(a), so that $\delta\omega$ in this case is dominated by a nonequilibrium effect. Noting that this structure is similar to the Fermi distribution function at finite temperatures, we expect that this nonequilibrium effect is similar to the thermal effect on a Fermi superfluid. Indeed, keeping this similarity in mind, when we introduce the effective temperature $T_{\mathrm{eff}} \equiv \delta\omega$ in the nonequilibrium case, one finds that $T_{\mathrm{eff}} > \Delta_{p_z:\mathrm{eq}}^{\uparrow\uparrow}$. This naturally explains why the p_z-wave superfluid state is destroyed in this case, that is, Cooper pairs are depaired by this "thermal" effect, as in the weak-coupling BCS state above the superfluid phase transition temperature.

As one increases the p_z-wave interaction strength, the smearing width $\delta\omega$ in the nonequilibrium case gradually becomes close to that in the equilibrium state, as shown in Fig. 5(b), around which the ratio $\langle\Delta_{p_z}^{\uparrow\uparrow}\rangle/\Delta_{p_z:\mathrm{eq}}^{\uparrow\uparrow}$ takes a maximum value [see Fig. 5(d)]. With further increasing the p_z-wave interaction strength, we see in Fig. 5(c) that $n_{\boldsymbol{p}}^{\uparrow}(t)$ again becomes different from the equilibrium result $\tilde{n}_{\boldsymbol{p}}^{\uparrow}$. As a result, the ratio $\langle\Delta_{p_z}^{\uparrow\uparrow}\rangle/\Delta_{p_z:\mathrm{eq}}^{\uparrow\uparrow}$ again becomes small, as shown in Fig. 5(d).

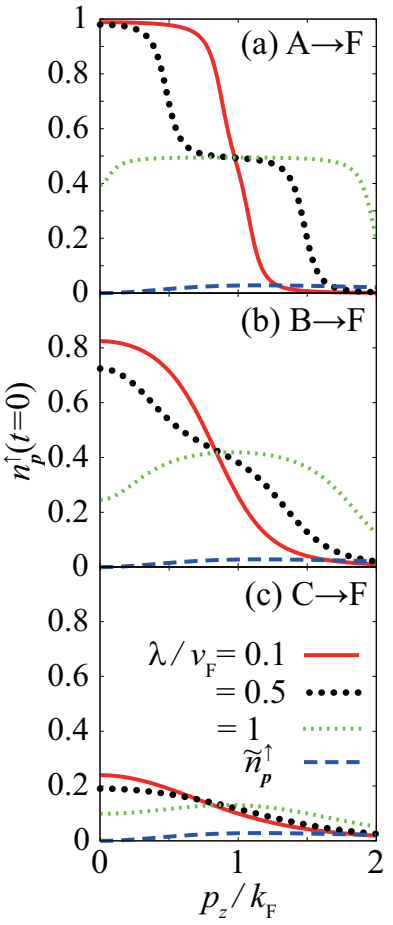

FIG. 7. Calculated atomic momentum distribution function $n^{\uparrow}_{\boldsymbol{p}}(t)$ with $\boldsymbol{p} = (0,0,p_z)$. $\tilde{n}^{\uparrow}_{\boldsymbol{p}}$ shows the equilibrium result when $(k_F^3 v_p)^{-1} = 6$ (case F). Since the time dependence of $n^{\uparrow}_{\boldsymbol{p}}(t)$ is weak, we only show the results at $t = 0$.

The above discussion is also applicable to the strong-coupling regime where the Fermi chemical potential μ in the equilibrium p_z-wave superfluid state is negative (the right side of the vertical dotted line in Fig. 4). When $(k_F^3 v_p)^{-1} = 6$ (case F), the equilibrium momentum distribution function $\tilde{n}^{\uparrow}_{\boldsymbol{p}}$ no longer has the Fermi-edge-like structure because of the negative chemical potential $\mu/\varepsilon_F \simeq -1.5$ [see Fig. 2(b1)]. In this case, Fig. 7 shows that the momentum distribution function $n^{\uparrow}_{\boldsymbol{p}}(t)$ relatively becomes similar to $\tilde{n}^{\uparrow}_{\boldsymbol{p}}$ with increasing the spin-orbit-coupling strength λ. Because of this, the ratio $\langle\Delta^{\uparrow\uparrow}_{p_z}\rangle/\Delta^{\uparrow\uparrow}_{p_z:\mathrm{eq}}$ is larger for a larger λ in the right side of the vertical dotted line in Figs. 4(b1)–4(b3).

In addition, when one increases $(k_F^3 v_p)^{-1}$ in the strong-coupling regime, the equilibrium momentum distribution function $\tilde{n}^{\uparrow}_{\boldsymbol{p}}$ spreads out more in momentum space, reflecting that the chemical potential approaches $\mu = -\infty$ in the strong-coupling limit. As a result, $n^{\uparrow}_{\boldsymbol{p}}(t)$ in this regime becomes increasingly different from $\tilde{n}^{\uparrow}_{\boldsymbol{p}}$ with increasing the p_z-wave interaction strength. This naturally explains why the ratio $\langle\Delta^{\uparrow\uparrow}_{p_z}\rangle/\Delta^{\uparrow\uparrow}_{p_z:\mathrm{eq}}$ decreases with increasing the p_z-wave interaction strength in the right side of the vertical dotted line in Figs. 4(b1)–4(b3).

These analyses indicate that in order to produce a large p_z-wave superfluid order parameter at $t \geqslant 0$, one should choose the equilibrium s-wave superfluid state ($t < 0$) so that the atomic momentum distribution function can be as similar as possible to that in the equilibrium p_z-wave superfluid state. Besides this, the fact that $n^{\uparrow}_{\boldsymbol{p}}(t) \neq \tilde{n}^{\uparrow}_{\boldsymbol{p}}$ seen in Figs. 5 and 6 means that the produced p_z-wave superfluid state is *not* in the ground state. In the current experimental stage [2–6], one cannot expect the relaxation of the produced p_z-wave superfluid state to the ground state within the short lifetime of a p-wave interacting Fermi gas. Thus, to study equilibrium thermodynamic properties of a p_z-wave superfluid Fermi gas in our approach, it would also be favorable to prepare the atomic momentum distribution in the initial s-wave superfluid state so as to be very similar to $\tilde{n}^{\uparrow}_{\boldsymbol{p}}$ in the equilibrium p_z-wave superfluid ground state. Actually, we need to find a way to prepare the p_z-wave-state-like *anisotropic* momentum distribution in the *isotropic* s-wave superfluid state for these purposes, which remains as our future problem.

Here, we discuss an alternative idea to obtain a nonvanishing p_z-wave superfluid order parameter deep inside the weak-coupling regime. The recent work [73] on the quench dynamics of a p-wave superfluid Fermi gas has shown that when a strong p-wave interaction is replaced by a weak p-wave one, the nonvanishing superfluid order parameter, whose value can be larger than that in the equilibrium case, is obtained. Indeed, when we solve TD-BdG equation (27) under the assumption that the system at $t < 0$ is in the equilibrium strong-coupling p_z-wave superfluid state [$(k_F^3 v_p)^{-1} = 8$], giving the initial state

$$\boldsymbol{\Phi}(\boldsymbol{p}, t=0) = \begin{pmatrix} \frac{E_p + \xi_p}{\sqrt{2E_p(E_p+\xi_p)}} \\ \frac{\Delta^{\uparrow\uparrow}_{p_z:\mathrm{eq}}(\boldsymbol{p})}{\sqrt{2E_p(E_p+\xi_p)}} \end{pmatrix} \tag{38}$$

(where $E_{\boldsymbol{p}} = \sqrt{\xi^2_{\boldsymbol{p}} + [\Delta^{\uparrow\uparrow}_{p_z:\mathrm{eq}}(\boldsymbol{p})]^2}$), we obtain the nonvanishing p_z-wave superfluid order parameter $\Delta^{\uparrow\uparrow}_{p_z}(t) \neq 0$, being larger than that in the equilibrium weak-coupling case, as shown in Fig. 8(a) [see also Fig. 2(b2)]. Then, one expects that our approach might also give a nonvanishing p_z-wave superfluid order parameter in the weak-coupling regime, when we replace the s-wave interaction by a strong p_z-wave one at $t = 0$, which is followed by the replacement of the strong p_z-wave interaction with a weak p_z-wave one at $t = t_0 > 0$, e.g., A → F → D. However, Fig. 8(b) shows that this idea actually does not work because the p_z-wave superfluid order parameter vanishes soon after the second manipulation. This is because, although a large p_z-wave superfluid order parameter appears when $0 \leqslant t \leqslant t_0$, the momentum distribution function $n^{\uparrow}_{\boldsymbol{p}}(t)$ is still similar to that in the initial s-wave state. As a result, the same mechanism as that discussed in Figs. 3(a1)–3(a3) works at $t = t_0$, leading to the vanishing of the p_z-wave superfluid order parameter seen in Fig. 8(b).

When we take into account the relaxation of the system to the equilibrium p_z-wave superfluid ground state beyond the present TD-BdG scheme, the momentum distribution function $n^{\uparrow}_{\boldsymbol{p}}(t)$ would become similar to $\tilde{n}^{\uparrow}_{\boldsymbol{p}}$ to some extent, during the period $0 \leqslant t \leqslant t_0$. Then, the situation becomes close to the case discussed in Ref. [73], which might give a nonvanishing

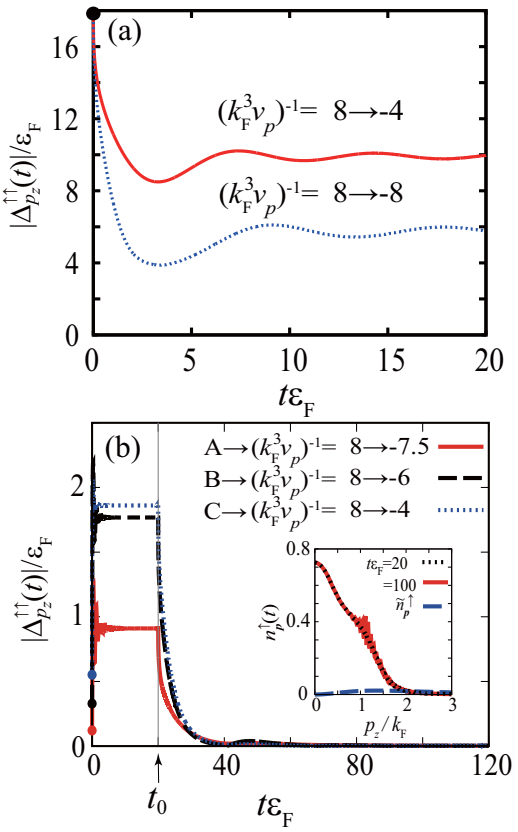

FIG. 8. (a) Quench dynamics of the magnitude of the p_z-wave superfluid order parameter $|\Delta_{p_z}^{\uparrow\uparrow}(t)|$. In this calculation, the system is initially in the equilibrium strong-coupling p_z-wave superfluid state with $(k_F^3 v_p)^{-1} = 8$. At $t = 0$, the interaction strength is suddenly tuned. (b) Time evolution of $|\Delta_{p_z}^{\uparrow\uparrow}(t)|$, when the s-wave interaction is replaced by the p-wave one at $t = 0$, which is followed by the interaction quench at $t\varepsilon_F = 20(= t_0\varepsilon_F)$. We take $\lambda/v_F = 0.5$ in the equilibrium s-wave state at $t < 0$. The inset shows the momentum distribution function $n_{\boldsymbol{p}}^{\uparrow}(t)$, with the dashed line the case of $|\Delta_{p_z}^{\uparrow\uparrow}(t)|$ in (b), where the equilibrium result $\tilde{n}_{\boldsymbol{p}}^{\uparrow}$ is in the case $(k_F^3 v_p)^{-1} = 8$.

p_z-wave superfluid order parameter even deep inside the weak-coupling regime. However, to confirm this expectation, we need to extend the present TD-BdG approach to include not only the relaxation effect, but also the three-body particle loss, which remains as our future problem.

Before ending this section, we comment on how to detect the p-wave superfluid state when $t \geqslant 0$. When the p-wave Cooper pairs with nonvanishing binding energy $E_{\rm bind}^{p\text{-wave}}(\neq 0)$ are really formed after the s-wave interaction is replaced by the p-wave one, this p-wave binding energy is expected to affect excitation properties of the system when $t \geqslant 0$. Thus, to detect $E_{\rm bind}^{p\text{-wave}}$, spectroscopic measurements, such as the radio-frequency spectroscopy [93] as well as Bragg spectroscopy [94], might be useful. For the superfluidity of the system, one idea is to observe the propagation of collective sound mode, which is characteristic of the superfluid phase, as has been done in an s-wave superfluid Fermi gas [95]. However, since the p-wave superfluid state discussed in this paper is in the nonequilibrium state, we need further analyses to assess to what extent these ideas work in the present case.

IV. SUMMARY

To summarize, we have discussed the time evolution of the p_z-wave superfluid order parameter, after an s-wave pairing interaction in an equilibrium spin-orbit-coupled s-wave superfluid Fermi gas is replaced by a p-wave interaction working between Fermi atoms in the same atomic hyperfine state (pseudospin-↑) at $t = 0$. Employing a time-dependent Bogoliubov–de Gennes (TD-BdG) equation at $T = 0$, we have examined how the p_z-wave superfluid order parameter $\Delta_{p_z}^{\uparrow\uparrow}(\boldsymbol{p},t \geqslant 0)$ is affected by the initial s-wave interaction strength ($t < 0$), the introduced p-wave interaction strength ($t \geqslant 0$), as well as the spin-orbit-coupling strength.

We showed that to obtain a large p_z-wave superfluid order parameter in this method, one should prepare the initial spin-orbit-coupled s-wave superfluid Fermi gas so that the atomic momentum distribution $n_{\boldsymbol{p}}^{\uparrow}(t = 0) \equiv n_{\boldsymbol{p}}^{\rm s}$ can be similar to that in the equilibrium p_z-wave superfluid state $\tilde{n}_{\boldsymbol{p}}^{\uparrow}$. In the p_z-wave weak-coupling regime where the Fermi chemical potential μ in the equilibrium p_z-wave superfluid state is positive, the p_z-wave superfluid order parameter was found to become large in the case when $n_{\boldsymbol{p}}^{\rm s}$ around the Fermi level ($p_z = \sqrt{2m\mu}$) is similar to that of $\tilde{n}_{\boldsymbol{p}}^{\uparrow}$. Although the Fermi edge does not exist in the p_z-wave strong-coupling regime where $\mu < 0$, we found that a larger p_z-wave superfluid order parameter is also obtained in the case when the overall structure of $n_{\boldsymbol{p}}^{\rm s}$ is relatively close to $\tilde{n}_{\boldsymbol{p}}^{\uparrow}$. The reason for the importance of the atomic momentum distribution in the initial spin-orbit-coupled s-wave superfluid state is that the overall structure of $n_{\boldsymbol{p}}^{\uparrow}(t)$ is passed down to that of nonequilibrium p_z-wave superfluid state $\tilde{n}_{\boldsymbol{p}}^{\uparrow}$ in the early stage of the time evolution ($t \geqslant 0$), where the relaxation effect as well as the three-body particle loss are not crucial.

At this stage, s-wave superfluid Fermi gases have only been realized in the absence of spin-orbit interaction. This implies that a spin-orbit interaction is not favorable to achieve the s-wave superfluid state. Thus, when we use our proposal, we should take a weak spin-orbit interaction, so as not to completely destroy the initial s-wave superfluid state. In this regard, slightly inside the p-wave weak-coupling regime may be suitable for this purpose because a relatively large p_z-wave superfluid order parameter can be obtained for a weak spin-orbit interaction [see Fig. 4(a1)]. Then, since the p_z-wave superfluid order parameter $\Delta_{p_z}^{\uparrow\uparrow}(\boldsymbol{p},t)$ grows much faster than the typical time scale of the three-body particle loss [$\tau_l = O(10\ {\rm ms})$], a p_z-wave superfluid state would be obtained, at least in the early stage of the time evolution after the p-wave interaction is turned on.

However, we should note that the TD-BdG formalism used in this paper ignores fluctuations in the p-wave Cooper channel, which becomes crucial when the p-wave interaction strength becomes strong. Since pairing fluctuations are considered to suppress the p-wave superfluid order parameter, it is an important issue to clarify this strong-coupling effect in order to evaluate the magnitude of the p-wave superfluid order parameter more quantitatively. Extension of the present TD-BdG approach to include p-wave pairing fluctuations is an important theoretical challenge.

In this paper, we have only considered the simplest single-component spin-orbit interaction, $\lambda p_z \sigma_x$. Since more complicated spin-orbit interactions, such as a two-component

one, also induce different types of p-wave pair amplitudes [47], it is an interesting future problem to see what happens in these cases after an appropriate p-wave interaction is switched on. In addition, it is known that a synthetic gauge field technique to produce a spin-orbit coupling also gives a Zeeman field term [41–45], which we have ignored in this paper, for simplicity. Inclusion of this realistic situation also remains as our future problem. Besides these, although we have simply assumed that the s-wave interaction is absent when $t \geqslant 0$, it may actually remain to some extent even after an external magnetic field is adjusted to a p-wave Feshbach resonance. In this case, the system may possess both the s-wave and p-wave superfluid order parameters, at least at $t = 0$. Furthermore, inclusions of relaxation effects as well as effects of three-body particle loss also remain to be solved. Since all of the current experiments toward the realization of a p-wave superfluid Fermi gas are facing the difficulty associated with the short lifetime of the system caused by a p-wave interaction, our results would provide an alternative route to reach this unconventional Fermi superfluid, avoiding this serious problem to some extent.

ACKNOWLEDGMENTS

We thank R. Hanai, H. Tajima, M. Matsumoto, and P. van Wyk for discussions. This work was supported by the KiPAS project at Keio University. D.I. was supported by a Grant-in-aid for Scientific Research from Japan Society for Promotion of Science (JSPS) in Japan (Grant No. 16K17773). Y.O. was supported by a Grant-in-aid for Scientific Research from JSPS in Japan (Grants No. 15H00840, No. 15K00178, No. 16K05503).

APPENDIX A: DERIVATION OF TD-BdG EQUATION (11)

We explain the outline of the derivation of TD-BdG equation (11) for an s-wave superfluid Fermi gas [54]. When the s-wave superfluid order parameter depends on t, the mean-field BCS Hamiltonian in Eq. (4) is also t dependent [$\equiv H_s^{\mathrm{MF}}(t)$]. In this case, the time evolution operator $\hat{U}(t)$ has the form

$$\hat{U}(t) = \mathcal{T}_t e^{-i\int_0^t dt' H_s^{\mathrm{MF}}(t')}, \tag{A1}$$

where $\mathcal{T}_t$ is the time-ordered product. Considering $c_{\boldsymbol{p},\sigma}(t) = \hat{U}^\dagger(t) c_{\boldsymbol{p},\sigma} \hat{U}(t)$ in the Heisenberg representation, we obtain the ordinary Heisenberg equation,

$$i\frac{\partial}{\partial t} c_{\boldsymbol{p},\sigma}(t) = \left[c_{\boldsymbol{p},\sigma}(t), H_s^{\mathrm{MF}}(t)\right]. \tag{A2}$$

TD-BdG assumes that $c_{\boldsymbol{p},\sigma}(t)$ has the same structure as the ordinary Bogoliubov transformation in the equilibrium case, except that the Bogoliubov amplitudes $\tilde{u}^\alpha_{\boldsymbol{p},\sigma}(t)$ and $\tilde{v}^\alpha_{\boldsymbol{p},\sigma}(t)$ in Eq. (14) depend on t. Then, substituting Eq. (14) into Eq. (A2), one reaches Eq. (11).

APPENDIX B: MOMENTUM DISTRIBUTION FUNCTION $n^\uparrow_{\boldsymbol{p}}(t \geqslant 0)$ IN THE PERPENDICULAR DIRECTION TO $\boldsymbol{p}_z$

Because $\Delta^{\uparrow\uparrow}_{p_z}(t)(\propto p_z)$ vanishes when $p_z = 0$, TD-BdG equation (27) in this case is reduced to

$$i\frac{\partial}{\partial t}\begin{pmatrix}\tilde{u}^\alpha_{\boldsymbol{p},\uparrow}(t)\\ \tilde{v}^\alpha_{\boldsymbol{p},\uparrow}(t)\end{pmatrix} = \begin{pmatrix}\varepsilon_{\boldsymbol{p}} & 0\\ 0 & -\varepsilon_{\boldsymbol{p}}\end{pmatrix}\begin{pmatrix}\tilde{u}^\alpha_{\boldsymbol{p},\uparrow}(t)\\ \tilde{v}^\alpha_{\boldsymbol{p},\uparrow}(t)\end{pmatrix}, \tag{B1}$$

which has the solution

$$\begin{pmatrix}\tilde{u}^\alpha_{\boldsymbol{p},\uparrow}(t)\\ \tilde{v}^\alpha_{\boldsymbol{p},\uparrow}(t)\end{pmatrix} = \begin{pmatrix}\tilde{u}^\alpha_{\boldsymbol{p},\uparrow}(0)e^{-i\varepsilon_{\boldsymbol{p}}t}\\ \tilde{v}^\alpha_{\boldsymbol{p},\uparrow}(0)e^{i\varepsilon_{\boldsymbol{p}}t}\end{pmatrix}. \tag{B2}$$

Equation (B2) gives the time-independent momentum distribution,

$$n^\uparrow_{\boldsymbol{p}}(t) = \frac{1}{2}\sum_{\alpha=\pm}|\tilde{v}^\alpha_{\boldsymbol{p},\uparrow}(t)|^2 = \frac{1}{2}\sum_{\alpha=\pm}|\tilde{v}^\alpha_{\boldsymbol{p},\uparrow}(0)|^2 = n^\uparrow_{\boldsymbol{p}}(0). \tag{B3}$$

[1] T. Yamaguchi, D. Inotani, and Y. Ohashi, J. Phys. Soc. Jpn. **86**, 013001 (2017).
[2] J. Levinsen, N. R. Cooper, and V. Gurarie, Phys. Rev. Lett. **99**, 210402 (2007).
[3] J. Levinsen, N. R. Cooper, and V. Gurarie, Phys. Rev. A **78**, 063616 (2008).
[4] M. Jona-Lasinio, L. Pricoupenko, and Y. Castin, Phys. Rev. A **77**, 043611 (2008).
[5] J. P. Gaebler, J. T. Stewart, J. L. Bohn, and D. S. Jin, Phys. Rev. Lett. **98**, 200403 (2007).
[6] J. Zhang, E. G. M. van Kempen, T. Bourdel, L. Khaykovich, J. Cubizolles, F. Chevy, M. Teichmann, L. Tarruell, S. J. J. M. F. Kokkelmans, and C. Salomon, Phys. Rev. A **70**, 030702(R) (2004).
[7] C. A. Regal, C. Ticknor, J. L. Bohn, and D. S. Jin, Phys. Rev. Lett. **90**, 053201 (2003).
[8] C. Ticknor, C. A. Regal, D. S. Jin, and J. L. Bohn, Phys. Rev. A **69**, 042712 (2004).
[9] K. Günter, T. Stöferle, H. Moritz, M. Köhl, and T. Esslinger, Phys. Rev. Lett. **95**, 230401 (2005).
[10] C. H. Schunck, M. W. Zwierlein, C. A. Stan, S. M. F. Raupach, W. Ketterle, A. Simoni, E. Tiesinga, C. J. Williams, and P. S. Julienne, Phys. Rev. A **71**, 045601 (2005).
[11] T. Nakasuji, J. Yoshida, and T. Mukaiyama, Phys. Rev. A **88**, 012710 (2013).
[12] F. Chevy, E. G. M. van Kempen, T. Bourdel, J. Zhang, L. Khaykovich, M. Teichmann, L. Tarruell, S. J. J. M. F. Kokkelmans, and C. Salomon, Phys. Rev. A **71**, 062710 (2005).
[13] C. A. Regal, C. Ticknor, J. L. Bohn, and D. S. Jin, Nature (London) **424**, 47 (2003).
[14] Y. Inada, M. Horikoshi, S. Nakajima, M. Kuwata-Gonokami, M. Ueda, and T. Mukaiyama, Phys. Rev. Lett. **101**, 100401 (2008).
[15] J. Fuchs, C. Ticknor, P. Dyke, G. Veeravalli, E. Kuhnle, W. Rowlands, P. Hannaford, and C. J. Vale, Phys. Rev. A **77**, 053616 (2008).
[16] C. A. Regal, M. Greiner, and D. S. Jin, Phys. Rev. Lett. **92**, 040403 (2004).
[17] M. W. Zwierlein, C. A. Stan, C. H. Schunck, S. M. F. Raupach, A. J. Kerman, and W. Ketterle, Phys. Rev. Lett. **92**, 120403 (2004).

[18] J. Kinast, S. L. Hemmer, M. E. Gehm, A. Turlapov, and J. E. Thomas, Phys. Rev. Lett. **92**, 150402 (2004).
[19] M. Bartenstein, A. Altmeyer, S. Riedl, S. Jochim, C. Chin, J. H. Denschlag, and R. Grimm, Phys. Rev. Lett. **92**, 203201 (2004).
[20] A. J. Leggett, Rev. Mod. Phys. **47**, 331 (1975).
[21] D. Vollhardt and P. Wölfle, *The Superfluid Phases of Helium 3* (Taylor and Francis, New York, 2002).
[22] M. Sigrist and K. Ueda, Rev. Mod. Phys. **63**, 239 (1991).
[23] G. R. Stewart, Rev. Mod. Phys. **56**, 755 (1984).
[24] A. P. Mackenzie and Y. Maeno, Rev. Mod. Phys. **75**, 657 (2003).
[25] M. Sinha and A. Sedrakian, Phys. Rev. C **91**, 035805 (2015).
[26] E. Timmermans, K. Furuya, P. W. Milonni, and A. K. Kerman, Phys. Lett. A **285**, 228 (2001).
[27] C. Chin, R. Grimm, P. Julienne, and E. Tiesinga, Rev. Mod. Phys. **82**, 1225 (2010).
[28] P. Nozières and S. Schmitt-Rink, J. Low Temp. Phys. **59**, 195 (1985).
[29] Y. Ohashi and A. Griffin, Phys. Rev. Lett. **89**, 130402 (2002).
[30] A. Perali, P. Pieri, G. C. Strinati, and C. Castellani, Phys. Rev. B **66**, 024510 (2002).
[31] Q. Chen, J. Stajic, S. Tan, and K. Levin, Phys. Rep. **412**, 1 (2005).
[32] M. Randeria, W. Zwerger, and M. Zwierlein, in *The BCS-BEC Crossover and the Unitary Fermi Gas*, edited by W. Zwerger (Springer-Verlag, Berlin, 2012), Chap. 1.
[33] S. Giorgini, L. P. Pitaevskii, and S. Stringari, Rev. Mod. Phys. **80**, 1215 (2008).
[34] I. Bloch, J. Dalibard, and W. Zwerger, Rev. Mod. Phys. **80**, 885 (2008).
[35] T.-L. Ho and R. B. Diener, Phys. Rev. Lett. **94**, 090402 (2005).
[36] Y. Ohashi, Phys. Rev. Lett. **94**, 050403 (2005).
[37] M. Iskin and C. A. R. Sá de Melo, Phys. Rev. Lett. **96**, 040402 (2006).
[38] M. Iskin and C. A. R. Sá de Melo, Phys. Rev. A **74**, 013608 (2006).
[39] D. Inotani, R. Watanabe, M. Sigrist, and Y. Ohashi, Phys. Rev. A **85**, 053628 (2012).
[40] D. Inotani and Y. Ohashi, Phys. Rev. A **92**, 063638 (2015).
[41] P. Wang, Z.-Q. Yu, Z. Fu, J. Miao, L. Huang, S. Chai, H. Zhai, and J. Zhang, Phys. Rev. Lett. **109**, 095301 (2012).
[42] L. W. Cheuk, A. T. Sommer, Z. Hadzibabic, T. Yefsah, W. S. Bakr, and M. W. Zwierlein, Phys. Rev. Lett. **109**, 095302 (2012).
[43] R. A. Williams, M. C. Beeler, L. J. LeBlanc, K. Jiménez-García, and I. B. Spielman, Phys. Rev. Lett. **111**, 095301 (2013).
[44] Z. Fu, L. Huang, Z. Meng, P. Wang, L. Zhang, S. Zhang, H. Zhai, P. Zhang, and J. Zhang, Nat. Phys. **10**, 110 (2014).
[45] L. Huang, P. Wang, P. Peng, Z. Meng, L. Chen, P. Zhang, and J. Zhang, Phys. Rev. A **91**, 041604(R) (2015).
[46] H. Hu, L. Jiang, X.-J. Liu, and H. Pu, Phys. Rev. Lett. **107**, 195304 (2011).
[47] T. Yamaguchi and Y. Ohashi, Phys. Rev. A **92**, 013615 (2015).
[48] Y. Endo, D. Inotani, R. Hanai, and Y. Ohashi, Phys. Rev. A **92**, 023610 (2015).
[49] D. Inotani, R. Hanai, and Y. Ohashi, Phys. Rev. A **94**, 043632 (2016).
[50] A. J. Leggett, in *Modern Trends in the Theory of Condensed Matter*, edited by A. Pekalski and J. Przystawa (Springer-Verlag, Berlin, 1980), p. 14.
[51] A. J. Leggett, *Quantum Liquids* (Oxford University Press, New York, 2006).
[52] C. A. R. Sá de Melo, M. Randeria, and J. R. Engelbrecht, Phys. Rev. Lett. **71**, 3202 (1993).
[53] M. Randeria, in *Bose-Einstein Condensation*, edited by A. Griffin, D. W. Snoke, and S. Stringari (Cambridge University Press, New York, 1995), p. 355.
[54] J. B. Ketterson and S. N. Song, *Superconductivity* (Cambridge University Press, Cambridge, 1998), Chap. 49.
[55] A. F. Andreev, Zh. Eksp. Teor. Fiz. **46**, 1823 (1964) [Sov. Phys. JETP **19**, 1228 (1964)].
[56] R. Kümmel, Z. Phys. **218**, 472 (1969).
[57] D. A. Takahashi, Phys. Rev. B **93**, 024512 (2016).
[58] R. A. Barankov, L. S. Levitov, and B. Z. Spivak, Phys. Rev. Lett. **93**, 160401 (2004).
[59] M. H. Szymańska, B. D. Simons, and K. Burnett, Phys. Rev. Lett. **94**, 170402 (2005).
[60] G. L. Warner and A. J. Leggett, Phys. Rev. B **71**, 134514 (2005).
[61] E. A. Yuzbashyan, O. Tsyplyatyev, and B. L. Altshuler, Phys. Rev. Lett. **96**, 097005 (2006).
[62] R. A. Barankov and L. S. Levitov, Phys. Rev. Lett. **96**, 230403 (2006).
[63] E. A. Yuzbashyan and M. Dzero, Phys. Rev. Lett. **96**, 230404 (2006).
[64] R. A. Barankov and L. S. Levitov, Phys. Rev. A **73**, 033614 (2006).
[65] A. Tomadin, M. Polini, M. P. Tosi, and R. Fazio, Phys. Rev. A **77**, 033605 (2008).
[66] E. A. Yuzbashyan, Phys. Rev. B **78**, 184507 (2008).
[67] V. Gurarie, Phys. Rev. Lett. **103**, 075301 (2009).
[68] C. K. Chung and C. K. Law, Phys. Rev. A **79**, 043611 (2009).
[69] C.-C. Chien and B. Damski, Phys. Rev. A **82**, 063616 (2010).
[70] M. S. Foster, V. Gurarie, M. Dzero, and E. A. Yuzbashyan, Phys. Rev. Lett. **113**, 076403 (2014).
[71] M. S. Foster, M. Dzero, V. Gurarie, and E. A. Yuzbashyan, Phys. Rev. B **88**, 104511 (2013).
[72] L. Austen, L. Cook, M. D. Lee, and J. Mur-Petit, Phys. Rev. A **87**, 023610 (2013).
[73] S. Yoon and G. Watanabe, arXiv:1512.09058v2.
[74] F. Setiawan, K. Sengupta, I. B. Spielman, and J. D. Sau, Phys. Rev. Lett. **115**, 190401 (2015).
[75] M. Dzero, A. A. Kirmani, and E. A. Yuzbashyan, Phys. Rev. A **92**, 053626 (2015).
[76] Y. Dong, L. Dong, M. Gong, and H. Pu, Nat. Commun. **6**, 6103 (2015).
[77] M. Lu, H. Liu, P. Wang, and X. C. Xie, Phys. Rev. B **93**, 064516 (2016).
[78] A. Roy, R. Dasgupta, S. Modak, A. Das, and K. Sengupta, J. Phys. Condens. Matter **25**, 205703 (2013).
[79] A. V. Andreev, V. Gurarie, and L. Radzihovsky, Phys. Rev. Lett. **93**, 130402 (2004).
[80] E. A. Yuzbashyan, M. Dzero, V. Gurarie, and M. S. Foster, Phys. Rev. A **91**, 033628 (2015).
[81] E. A. Yuzbashyan and O. Tsyplyatyev, Phys. Rev. B **79**, 132504 (2009).
[82] G. Tonini, F. Werner, and Y. Castin, Eur. Phys. J. D **39**, 283 (2006).
[83] K. J. Challis, R. J. Ballagh, and C. W. Gardiner, Phys. Rev. Lett. **98**, 093002 (2007).
[84] R. G. Scott, F. Dalfovo, L. P. Pitaevskii, and S. Stringari, Phys. Rev. A **86**, 053604 (2012).

[85] S. Hannibal, P. Kettmann, M. D. Croitoru, A. Vagov, V. M. Axt, and T. Kuhn, Phys. Rev. A **91**, 043630 (2015).

[86] The 4×4 Hamiltonian $\hat{H}_s^{\text{TD-BdG}}(t)$ in Eq. (12) actually has four eigenstates. However, because of the particle-hole symmetry, their eigenenergies can always be classified as $(E_{\boldsymbol{p}}^+, -E_{\boldsymbol{p}}^+)$ and $(E_{\boldsymbol{p}}^-, -E_{\boldsymbol{p}}^-)$. Using this symmetry property, as usual, we construct the Bogoliubov transformation in Eq. (14) by only using the two positive-energy solutions ($\alpha = \pm$).

[87] P. G. de Gennes, *Superconductivity of Metals and Alloys* (Addison-Wesley, New York, 1989), Chap. 5.

[88] R. Liao, F. Popescu, and K. Quader, Phys. Rev. B **88**, 134507 (2013).

[89] The cutoff momentum p_0 is related to the inverse effective range $k_{\text{eff}} = -(\pi p_0^2/m^2)\sum_{\boldsymbol{p}}(\boldsymbol{F}_{\boldsymbol{p}}^2/\varepsilon_{\boldsymbol{p}}^2) - 2/(p_0^2 v_p)$ [35,37,38]. Experimentally, this quantity has been observed as $k_{\text{eff}} = -0.02 a_{\text{B}}^{-1}$ in a ^{40}K Fermi gas [8] and $k_{\text{eff}} = -0.05 a_{\text{B}}^{-1}$ in a ^{6}Li Fermi gas [11] (where a_{B} is the Bohr radius). Using the typical value $k_{\text{F}}^{-1} \sim 100$ nm in an ultracold Fermi gas, one has $p_0 \sim 10^2 k_{\text{F}}$. However, we take $p_0 = 10 k_{\text{F}} \ll 10^2 k_{\text{F}}$ in this paper because of computational problems. While this smaller p_0 does not qualitatively alter our conclusions, it is known to quantitatively affect the magnitude of the equilibrium p-wave superfluid order parameter [37,38].

[90] H.-J. Miesner, D. M. Stamper-Kurn, M. R. Andrews, D. S. Durfee, S. Inouye, and W. Ketterle, Science **279**, 1005 (1998).

[91] The p_z-wave superfluid order parameter $\Delta_{p_z}^{\uparrow\uparrow}(t)$ is a complex function, so that we plot the absolute value of this quantity in Fig. 3. In the TD-BdG scheme, even in the equilibrium state, it is complex as $\Delta_{p_z}^{\uparrow\uparrow}(t) = e^{-2i\mu t}\Delta_{p_z:\text{eq}}^{\uparrow\uparrow}$.

[92] The time interval $t\varepsilon_{\text{F}} = [50, 100]$ in Eq. (35) is simply chosen so as to roughly estimate the averaged magnitude of $\Delta_{p_z}^{\uparrow\uparrow}(t)$ in the long-time region ($t\varepsilon_{\text{F}} \gg 1$). Actually, one still sees in, for example, Fig. 3(b1) remarkable time dependence of $\Delta_{p_z}^{\uparrow\uparrow}(t)$ in this time domain. However, even in this case, $\langle\Delta_{p_z}^{\uparrow\uparrow}\rangle$ in Eq. (35) is still convenient to see the order of $\Delta_{p_z}^{\uparrow\uparrow}(t\varepsilon_{\text{F}} \gg 1)$.

[93] C. Chin, M. Bartenstein, A. Altmeyer, S. Riedl, S. Jochim, J. H. Denschlag, and R. Grimm, Science **305**, 1128 (2004).

[94] P. Zou, E. D. Kuhnle, C. J. Vale, and H. Hu, Phys. Rev. A **82**, 061605 (2010).

[95] D. E. Miller, J. K. Chin, C. A. Stan, Y. Liu, W. Setiawan, C. Sanner, and W. Ketterle, Phys. Rev. Lett. **99**, 070402 (2007).